Refereed Proceedings

The 13th International Conference on Fluidization - New Paradigm in Fluidization Engineering

Engineering Conferences International *Year* 2010

GAS-SOLID FLUIDIZATION IN A MICROFLUIDIC CHANNEL

Fei Wang* L S Fan†

*The Ohio State University

†The Ohio State University, fan@chbmeng.ohio-state.edu

GAS-SOLID FLUIDIZATION IN A MICROFLUIDIC CHANNEL

Fei Wang and Liang-Shih Fan*

William G. Lowrie Department of Chemical and Biomolecular Engineering
The Ohio State University
Columbus, Ohio 43210, USA

*To whom correspondence should be addressed (fan@chbmeng.ohio-state.edu)

ABSTRACT

Experimental studies using a high speed digital camera are conducted to examine gas-solid fluidization in microfluidic channels (3mmX3mm and 2mmX3mm). The experimental results indicate the significant channel wall effects on the hydrodynamic properties including bed expansion and regime transition velocities. These properties are analyzed and discussed in the context of correlation equations reported for large fluidized beds.

INTRODUCTION

Multiphase flow systems are widely encountered in industrial operations such as fluidized beds, bubble columns, slurry bubble columns, and solid-liquid and solid pneumatic conveying. Fluidized beds can provide good mass and heat transfer characteristics, temperature homogeneity, high flowability of particles, and high mixing rates between solid particles and gas. Gas-solid fluidized beds, in which solid particles are fluidized by a gas injected from the bottom distributor of the bed, have been used extensively in chemical, petrochemical, metallurgical, food, and pharmaceutical industries. Fluidized bed reactors for these industrial applications are large in scale. Further, much of the fundamental research on fluidization properties has its underlining interest in interpreting or being useful to designing industrial fluidized systems (Ergun (1), Wen and Yu (2), Geldart (3), Yerushalmi and Cankurt (4), Abrahamsen and Geldart (5, 6), Molerus (7), Grace (8), Cai et al. (9), Fan and Zhu (10)). Miniaturization of chemical reactors provides unique operational characteristics and applications counter to the regular/large reactor systems. Specifically, Micro-reactors yield excellent interfacial contact phenomena and hence a high-rate transport process and global reaction kinetics (Maharrey and Miller (11), Kolb and Hessel (12)). Studies of micro-fluidized beds with an inner diameter of 1.2 centimeter to a few centimeters and a bed height of a few centimeters were reported in the literature (Liu et al. (13)). With further decrease in the fluidized bed size to the microfluidic channel range which is commonly considered in the microfluidic field for gas-liquid, liquid-solid, or liquid-liquid flows (Potic et al. (14), Gunther and Jensen (15)), the wall effect on fluidization properties would further enhance. Characteristics such as bubble/slug shape and size, holdup, and liquid velocity distribution in gas-liquid and liquid-solid microfluidic channels have been studied in the past decade

(Waelchli and von Rohr (16), Yu et al. (17)). Little is known of gas-solid fluidization conducted in microfluidic channels.

In this study, gas-solid fluidization in a microfluidic channel both in the gravitational force field and in a centrifugal force field is conducted. The visualization of the dynamic behavior of fluidization in the microfluidic channel is carried out. The state of gas-solid fluidization, regime transition and bed expansion in the microfluidic channels are examined. Comparisons of its behavior with that in the larger gas-solid fluidized beds are made.

EXPERIMENTAL SETUP

Figure 1 presents the schematic diagram of the microfluidic gas-solid fluidization system developed in this study. It consists of a Plexiglass rectangular microfluidic channel (3mmX3mm and 2mmX3mm), a syringe and syringe pump that provides the fluidizing gas to establish required superficial gas velocity, a Photron FASTCAM PCI high-speed CCD camera with a Navitar ZOOM 7000 lens and a close-up lens set, a Photron FASTCAM data processing system to record the images, a light unit to provide illumination for photography. The distributor in the microfluidic channel is made of a porous plate with a pore size of 20 μm and a fractional free area of 60%. The total length of the microfluidic channel is 180 mm. FCC powders with a density of 1400 kg/m^3 and a mean diameter of 60 μm are used as the solids. The particles are sieved and particles with sizes above 75 μm are removed. The gas-solid fluidization behavior in the microfluidic channel is investigated both in the gravitational force field and in a centrifugal force field. For the study in the gravitational force field, the microfluidic channel is placed vertically as shown in Figure 1. The high speed camera is placed in front of the microfluidic channel to capture the dynamic images at a speed of 500 frames per second. For the study in the centrifugal force field as shown in Figure 2, the microfluidic channel is mounted on a rotating horizontal disk with a controlled rotational speed to provide different centrifugal forces that exerted on the particles in the channel. The gas supply line is placed on the unmoving outer shell of the system. An intricate bearing system is used to connect the rotating gas inlet tube with the unmoving supply. The fluidizing gas flows into the microfluidic channel towards the center of the disk and fluidizes the particles by overcoming the centrifugal force. The high speed digital camera is placed above the system to capture the dynamic behavior of the particle fluidization occurring in the channel at a speed of 500 frames per second. Since the camera is fixed, the fluidization images can only be captured when the microfluidic channel is in line with the lens during its rotation.

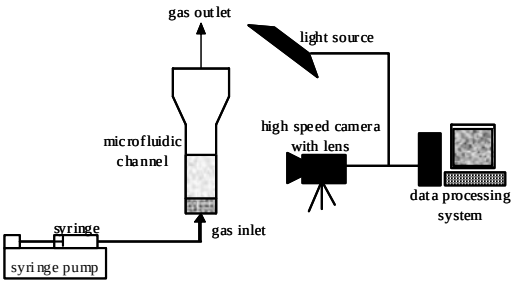

Figure 1. Schematic diagram of the microfluidic gas-solid fluidization system

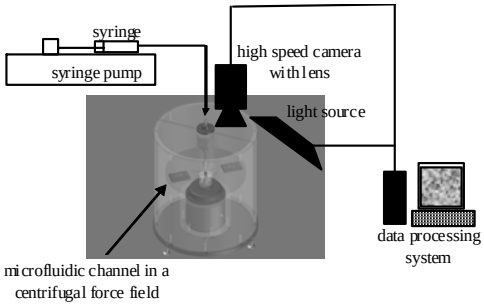

Figure 2. Microfluidic gas-solid fluidization system in a centrifugal force field

RESUTLS AND DISCUSSION

Voidage, U_{mf} and U_{mb} in the Microfluidic Channel

The overall voidage, $\varepsilon_{overall}$, dense phase voidage, ε_{dense}, and bubble fractional holdup, ε_{bubble}, in the microfluidic channel were obtained by the bed collapse experiments (Dry et al. (18), Yang et al. (19)). During the bed collapse experiments, the syringe pump was rapidly stopped and the fluidizing gas was cut off. The bed height was captured by the images from the high speed camera. Figure 3 shows the dynamic bed height in the 3mmX3mm microfluidic channel from the bed collapse experiments. The superficial gas velocity, U_g, in the microfluidic channel was 55 mm/s. H_f is the average bed height before the gas was cut off. H_{dense} is the height of the dense phase. $\varepsilon_{overall}$, ε_{dense}, and ε_{bubble} were calculated from Equation (1)-(3):

$$\varepsilon_{overall} = 1 - \frac{w}{AH_f \rho_p} \tag{1}$$

$$\varepsilon_{dense} = 1 - \frac{w}{AH_{dense} \rho_p} \tag{2}$$

$$\varepsilon_{bubble} = \varepsilon_{overall} - \varepsilon_{dense} \tag{3}$$

where A is the cross-sectional area of the microfluidic channel; w is the weight of the particles in the microfluidic channel; and ρ_p is the particle density. $\varepsilon_{overall}$, ε_{dense}, and ε_{bubble} at different superficial gas velocities in the 3 mm microfluidic channel are shown in Figure 4.

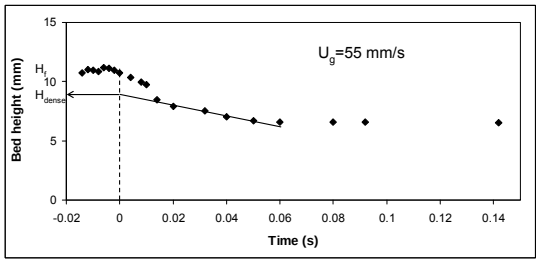

Figure 3. Dynamic bed height in the 3mmX3mm microfluidic channel from the bed collapse experiment

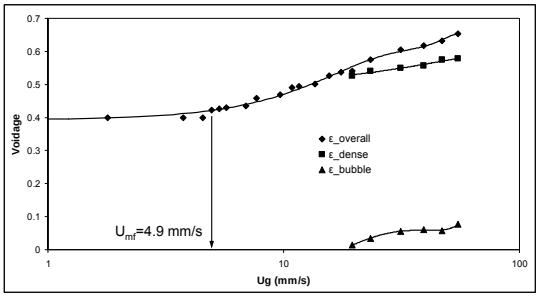

Figure 4. Fluidization map for the 3mmX3mm microfluidic channel

It is seen that $\varepsilon_{overall}$, ε_{dense}, and ε_{bubble} all increase with an increase in the superficial gas velocity. The minimum fluidization velocity, U_{mf}, and the minimum bubbling velocity, U_{mb}, are 4.9 mm/s and ~13.5 mm/s, respectively, in the 3mmX3mm microfluidic channel for the sieved FCC particles. U_{mf} and U_{mb} are 5.6 mm/s and ~14.5 mm/s, respectively, in the 2mmX3mm microfluidic channel. Table 1 shows the comparison of U_{mf} in the microfluidic channel and the regular/large fluidized beds. It is seen that the minimum fluidization velocity in the microfluidic channel is 3-5 times of that in the regular fluidized beds. Table 2 shows the comparison of U_{mb} in the microfluidic channel and the regular fluidized beds. The minimum bubbling velocity in the microfluidic channel is ~3 times of that in the regular fluidized beds.

Table 1. Comparison of minimum fluidization velocity in the microfluidic channel and the correlations from literatures

	3mmX3mm Microfluidic Channel	2mmX3mm Microfluidic Channel	Rowe and Henwood (20)	Wen and Yu (2)	Simone and Harriott (21)	Grace (22)
U_{mf} (mm/s)	4.9	5.6	1.7	1.3	1	1.6

Table 2. Comparison of minimum bubbling velocity in the microfluidic channel and the correlations from literatures

	3mmX3mm Microfluidic Channel	2mmX3mm Microfluidic Channel	Geldart (3)	Geldart and Abrahansen (23)
U_{mb} (mm/s)	~13.5	~14.5	5.3	4.4

The significant increase of U_{mf} and U_{mb} is due to the extra pressure drop on the particles induced by the wall effect in the microfluidic channel. Similar results were obtained using channels of 1.2 cm, 2.0 cm and 3.2 cm ID with sands by Liu et al. (13).

Bubble Size

Figure 5 shows a snapshot of a rising micro bubble in the microfluidic channel with a U_g of 39 mm/s. A maximum stable bubble size in the regular gas-solid fluidized beds for Group A particles has been studied intensively in the literature. Figure 6 shows the comparison of the experimental results of the maximum stable bubble size at 5 mm above the distributor in the microfluidic channel and the predicted based on correlation equations for regular fluidized beds by Rowe (24), Werther (25), Darton et al. (26) and Cai et al. (27). It is seen that the experimental results of the bubble size in the microfluidic channel are reasonably comparable, though slightly lower, to the predictions by Darton et al. (26) and Cai et al. (27). The experimental results in Figure 6 indicate that the correlations by Rowe (24) and Werther (25) are not predictive for the bubble size in the microfluidic channel. The bubble size increases with the superficial gas velocity in the microfluidic channel.

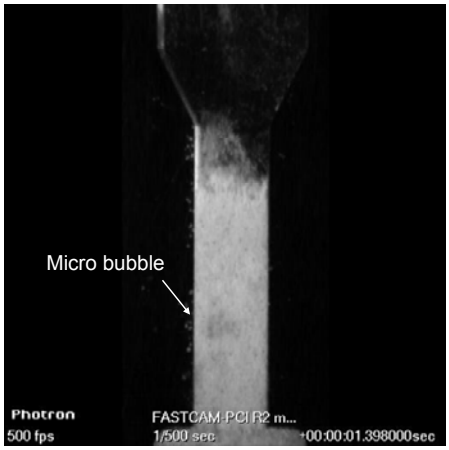

Figure 5. A rising bubble in the 3mmX3mm microfluidic channel

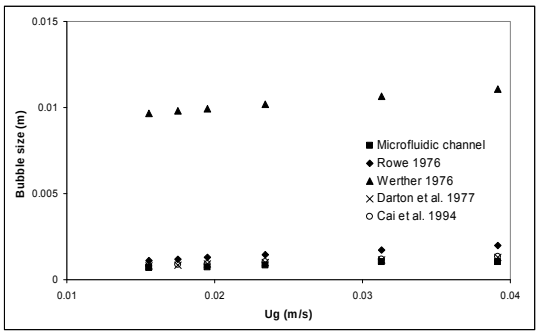

Figure 6. Comparison of bubble sizes in the 3mmX3mm microfluidic channel and

the correlations from literatures

Slugging

The minimum gas velocity and minimum bed height required for slugging in the 3mmX3mm microfluidic channel can be calculated as 12 mm/s based on the Stewart and Davidson criterion (Stewart and Davidson (28)) and 486 mm based on the Baeyens and Geldart criterion (Baeyens and Geldart (29)). However, the experimental results show that the slugging occurs at a gas velocity of 31 mm/s and a bed height of 12 mm in the 3mmX3mm microfluidic channel and at a gas velocity of 29 mm/s and a bed height of 8 mm in the 2mmX3mm microfluidic channel. The experimental results indicate that the Stewart and Davidson criterion and the Baeyens and Geldart criterion are not predictive for the microfluidic channels. Figure 7 (a) and (b) depict two snapshots of slugs in the 3mmX3mm and 2mmX3mm microfluidic channels. The slugs in these two snapshots are round-nosed slugs. Wall slugs are also observed due to large d_p/D ratio in the microfluidic channels, where d_p and D are the particle diameter and channel ID, respectively.

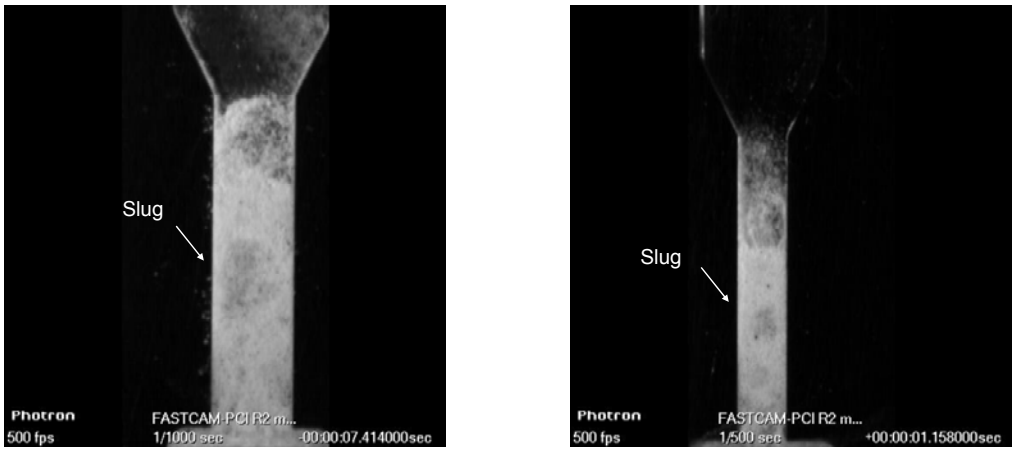

(a) (b)

Figure 7. Snapshots of slugs in the microfluidic channels: (a) U_g=55 mm/s; channel size=3mmX3mm; (b) U_g=58 mm/s; channel size=2mmX3mm

Fluidization in a Centrifugal Force Field

To study the effect due to the centrifugal force field, the microfluidic channel is mounted on the rotating horizontal disk. The fluidizing gas flows into the microfluidic channel towards the center of the disk and fluidizes the particles by overcoming the centrifugal force. Since the camera above the disk is fixed, the fluidization images can only be captured when the microfluidic channel is underneath the lens during its rotation. Figure 8 presents snapshots of gas-solid fluidization in a 3mmX3mm microfluidic channel in the centrifugal force field with an angular velocity, ω, of 287 r/m and a U_g of 15.5 mm/s. The accelerations near the distributor and at the free surface of the bed in the microfluidic channel provided by the rotating horizontal disk are 1.77 m/s^2 and 1.63 m/s^2, respectively. The bubble size increases with the bed height due to bubble coalescence and reduction of the acceleration. A large amount of bubbles are close to the wall region when moving towards the outlet of the channel due to the significant wall effect in the microfluidic channel and the small body force exerted on the particles in the horizontal direction.

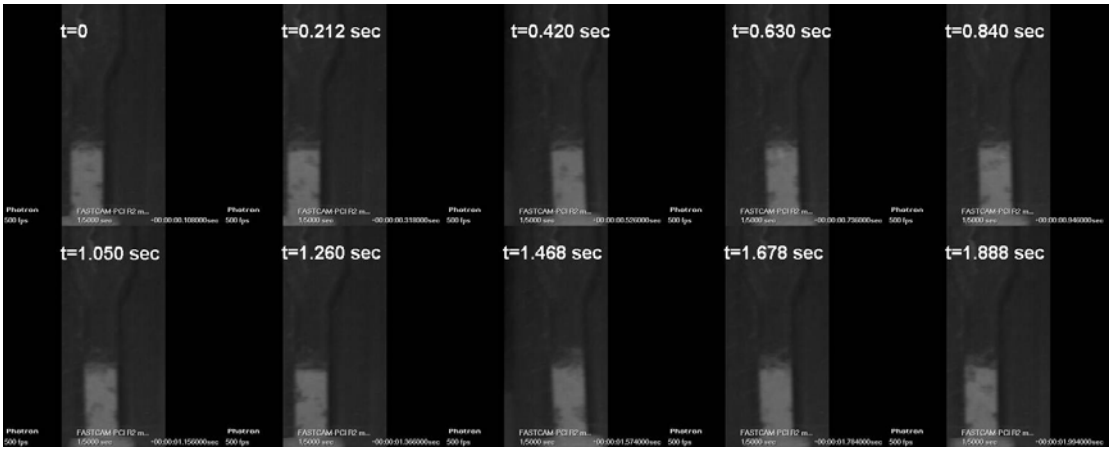

Figure 8 Snapshots of gas-solid fluidization in a 3mmX3mm microfluidic channel in the centrifugal force field: ω=287 r/m; U_g=15.5 mm/s

CONCLUDING REMARKS

Gas-solid fluidization in microfluidic channels (3mmX3mm and 2mmX3mm) is examined. The gas-solid fluidization states, regime transition and bed expansion in the microfluidic channels are investigated and compared with those in the regular large gas-solid fluidized beds through visualization. U_{mf} and U_{mb} in the microfluidic channels are larger than that in the regular fluidized beds. The significant increase of U_{mf} and U_{mb} is due to the extra pressure drop on the particles exerted by the wall in the microfluidic channel. The bubble size increases with the superficial gas velocity in the microfluidic channel and is comparable to the predictions by Darton et al. (26) and Cai et al. (27). The slugging phenomenon commonly occurs in microfluidic channels due to large d_p/D ratio. The experimental results indicate that the Stewart and Davidson criterion and the Baeyens and Geldart criterion are unpredictive for the microfluidic channels. Both round-nosed slugs and wall slugs are observed in the microfluidic channel. Gas-solid fluidization in a microfluidic channel in a centrifugal force field is also studied. The bubble size increases with the bed height due to bubble coalescence and reduction of the centrifugal force. A large amount of the bubbles are close to the wall region when moving towards the outlet of the microfluidic channel due to the wall effect and the small body force exerted on the particles in the horizontal direction.

ACKNOWLEDGEMENT

The assistance of Paul Green and Thomas Yeh in the fabrication of the gas-solid microfluidic system is gratefully acknowledged.

NOTATION

A	cross-sectional area of the microfluidic channel
d_p	particle diameter
D	channel ID
H_{dense}	height of the dense phase
H_f	average bed height before cutting off the gas
U_g	superficial gas velocity
U_{mb}	minimum bubbling velocity

U_{mf} minimum fluidization velocity
w weight of the particles in the microfluidic channel
ε_{bubble} bubble fractional holdup
ε_{dense} dense phase voidage
$\varepsilon_{overall}$ overall voidage
ρ_p particle density
ω angular velocity

REFERENCES

(1) Ergun, S., Fluid flow through packed columns. *Chemical Engineering Progress* **1952,** *48*, 89-94.
(2) Wen, C. Y.; Yu, Y. H., A Generalized Method for Predicting Minimum Fluidization Velocity. *Aiche Journal* **1966,** *12*, 610-612.
(3) Geldart, D., Types of Gas Fluidization. *Powder Technology* **1973,** *7*, 285-292.
(4) Yerushalmi, J.; Cankurt, N. T., Further studies of the regimes of fluidization. *Powder Technology* **1979,** *24*, 187-205.
(5) Abrahamsen, A. R.; Geldart, D., Behavior of Gas-Fluidized Beds of Fine Powders .1. Homogeneous Expansion. *Powder Technology* **1980,** *26*, 35-46.
(6) Abrahamsen, A. R.; Geldart, D., Behavior of Gas-Fluidized Beds of Fine Powders .2. Voidage of the Dense Phase in Bubbling Beds. *Powder Technology* **1980,** *26*, 47-55.
(7) Molerus, O., Interpretation of Geldart's type A, B, C, and D powders by taking into account interparticle cohesion forces. *Powder technology* **1982,** *33*, 81-87.
(8) Grace, J. R., Contacting modes and behavior classification of gas-solid and other two-phase suspensions. *Can. J. Chem. Eng.* **1986,** *64*, 353-363.
(9) Cai, P.; Chen, S. P.; Jin, Y.; Yu, Z. Q.; Wang, Z. W., Effect of operating temperature and pressure on the transition from bubbling to turbulent fluidization. *AIChE Symp. Ser.* **1989,** *85*, 37-43.
(10) Fan, L.-S.; Zhu, C., *Principles of gas-solid flows*. Cambridge University Press: Cambridge ; New York, 1998; 557 p.
(11) Maharrey, S. P.; Miller, D. R., Quartz capillary microreactor for studies of oxidation in supercritical water. *AIChE Journal* **2001,** *47*, 1203-1211.
(12) Kolb, G.; Hessel, V., Micro-structured reactors for gas phase reactions. *Chemical Engineering Journal* **2004,** *98*, 1-38.
(13) Liu, X. H.; Xu, G. W.; Gao, S. Q., Micro fluidized beds: Wall effect and operability. *Chemical Engineering Journal* **2008,** *137*, 302-307.
(14) Potic, B.; Kersten, S. R. A.; Ye, M.; van der Hoef, M. A.; Kuipers, J. A. M.; van Swaaij, W. P. M., Fluidization with hot compressed water in micro-reactors. *Chemical Engineering Science* **2005,** *60*, 5982-5990.
(15) Gunther, A.; Jensen, K. F., Multiphase microfluidics: from flow characteristics to chemical and materials synthesis. *Lab on a Chip* **2006,** *6*, 1487-1503.
(16) Waelchli, S.; von Rohr, P. R., Two-phase flow characteristics in gas-liquid microreactors. *International Journal of Multiphase Flow* **2006,** *32*, 791-806.
(17) Yu, Z.; Hemminger, O.; Fan, L.-S., Experiment and lattice Boltzmann simulation of two-phase gas-liquid flows in microchannels. *Chemical Engineering Science* **2007,** *62*, 7172-7183.
(18) Dry, R. J.; Judd, M. R.; Shingles, T., two-phase theory and fine powders. *Powder Technology* **1983,** *34*, 213-223.

(19) Yang, Z. P.; Tung, Y. K.; Kwauk, M. S., Characterizing Fluidization by the Bed Collapsing Method. *Chemical Engineering Communications* **1985,** *39*, 217-232.
(20) Rowe, P. N.; Henwood, G. A., Drag forces in a hydraulic model of a fluidized bed, Part 2. *Trans. Inst. Chem. Eng.* **1961,** *39*, 157-180.
(21) Simone, S.; Harriott, P., Fluidization of Fine Powders with Air in the Particulate and the Bubbling Regions. *Powder Technology* **1980,** *26*, 161-167.
(22) Grace, J. R., Fluidized-Bed Hydrodynamics. In *Handbook of Multiphase Systems*, Hetsroni, G., Ed. Hemisphere: Washington, 1982; pp 5-64.
(23) Geldart, D.; Abrahamsen, A. R., Homogeneous Fluidization of Fine Powders Using Various Gases and Pressures. *Powder Technology* **1978,** *19*, 133-136.
(24) Rowe, P. N., Prediction of Bubble-Size in a Gas-Fluidized Bed. *Chemical Engineering Science* **1976,** *31*, 285-288.
(25) Werther, J., Bubble growth in large diameter fluidized beds. In *Fluidization Technology*, Keairns, D. L., Ed. Hemisphere: Washington, 1976; pp 215-235.
(26) Darton, R. C.; Lanauze, R. D.; Davidson, J. F.; Harrison, D., Bubble-Growth Due to Coalescence in Fluidized-Beds. *Transactions of the Institution of Chemical Engineers* **1977,** *55*, 274-280.
(27) Cai, P.; Schiavetti, M.; Demichele, G.; Grazzini, G. C.; Miccio, M., Quantitative Estimation of Bubble-Size in Pfbc. *Powder Technology* **1994,** *80*, 99-109.
(28) Stewart, P. S. B.; Davisdson, J. F., Slug flow in fluidised beds. *Powder Technology* **1967,** *1*, 61-80.
(29) Baeyens, J.; Geldart, D., Investigation into Slugging Fluidized-Beds. *Chemical Engineering Science* **1974,** *29*, 255-265.